Intersegment Hydrogen Bonds as Possible Structural Determinants of the N/Q/R Site in Glutamate Receptors

Denis B. Tikhonov, Boris S. Zhorov, and Lev G. Magazanik
Sechenov Institute of Evolutionary Physiology and Biochemistry of the Russian Academy of Sciences, St. Petersburg 194223, Russia

ABSTRACT Specific electrophysiological and pharmacological properties of ionic channels in NMDA, AMPA, and kainate subtypes of ionotropic glutamate receptors (GluRs) are determined by the Asn (N), Gln (Q), and Arg (R) residues located at homologous positions of the pore-lining M2 segments (the N/Q/R site). Presumably, the N/Q/R site is located at the apex of the reentrant membrane loop and forms the narrowest constriction of the pore. Although the shorter Asn residues are expected to protrude in the pore to a lesser extent than the longer Gln residues, the effective dimension of the NMDA channel (corresponding to the size of the largest permeant organic cation) is, surprisingly, smaller than that of the AMPA channel. To explain this paradox, we propose that the N/Q/R residues form macrocyclic structures (rings) stabilized by H-bonds between a NH_2 group in the side chain of a given M2 segment and a C═O group of the main chain in the adjacent M2 segment. Using Monte Carlo minimization, we have explored conformational properties of the rings. In the Asn, but not in the Gln ring, the side-chain oxygens protruding into the pore may facilitate ion permeation and accept H-bonds from the blocking drugs. In this way, the model explains different electrophysiological and pharmacological properties of NMDA and non-NMDA GluR channels. The ring of H-bonded polar residues at the pore narrowing resembles the ring of four Thr^{75} residues observed in the crystallographic structure of the KcsA K^+ channel.

INTRODUCTION

L-glutamate is the main excitatory neurotransmitter in the central nervous system of vertebrates. It activates ionotropic glutamate receptors (GluRs), transmembrane proteins that belong to the superfamily of ligand-gated ion channels (Seeburg, 1993; Westbrook, 1994). GluRs are subdivided into three subtypes according to their predominant specific agonist: NMDA, AMPA, and kainate. NMDA receptors are heterooligomers composed of NR1 and NR2A–NR2D subunits. AMPA receptors (subunits GluR1–GluR4) and kainate receptors (subunits GluR5–GluR7, KA-1, KA-2) exist in both homooligomeric and heterooligomeric forms (see Hollmann and Heinemann, 1994). The central ion pore in GluRs is lined by M2 segments (M2s) from the receptor subunits with possible involvement of other segments (Mori et al., 1992; Burnashev et al., 1992b; Kohler et al., 1993; Ferrer-Montiel et al., 1995).

M2s of the nicotinic acetylcholine receptor, the best-studied protein in the superfamily, are transmembrane α-helices (see Galzi and Changeux, 1995) that may be kinked in their middle part (Unwin, 1995). In contrast, M2s of GluRs have a form of a membrane-diving loop with the ends at the cytoplasmic side. This model was initially proposed for AMPA and kainate receptors for which N-glycosylation experiments revealed only three transmembrane segments (Wo and Oswald, 1994; Hollmann et al., 1994). The cysteine-scanning analysis of M2s in NR1 and NR2A subunits of NMDA receptor has supported the model with the reentrant membrane loops (Kuner et al., 1996). M2 in NR1 subunit was demonstrated to form four helical turns at the N-end, but no regular structure was found for M2 in NR2 subunit (see Table 1).

Ion conductance, ion selectivity, and blockade of GluRs are governed by residues presumably located at the apex of the M2 loop that is called the N/Q/R site. The NMDA receptor subunits have Asn (N) residue at the N/Q/R site, whereas non-NMDA (AMPA and kainate) receptors have Gln (Q) residue at this site, with the exception of GluR2, GluR5, and GluR6 subunits (Table 1). In these subunits, Gln is replaced by Arg (R) as a result of mRNA editing (Keinanen et al., 1990). The effect of the N/Q/R site on the channel properties has been intensively studied in wild-type and recombinant receptors. It was found that the N/Q/R site controls the effective diameter of the open pore, as estimated from the diameter of the largest permeating organic cation (Villarroel et al., 1995, Burnashev et al., 1996; Wollmuth et al., 1996). These data provide evidence that the N/Q/R site forms the most narrow channel constriction in GluRs. It should be noted, however, that other explanations could not be ruled out. For example, the N/Q/R site may control the channel properties by indirectly affecting the structure of the pore region.

Substitution of Asn in the N/Q/R site of NMDA receptors by Gln yielded channels with some properties resembling those of the non-NMDA receptor channels (Burnashev et al., 1992b; Mori et al., 1992) and vice versa (Ferrer-Montiel et al., 1995). Ion channel properties of AMPA receptors strongly depend on the subunit composition. Ion channel

Received for publication 30 November 1998 and in final form 16 June 1999.

Address reprint requests to Dr. D. B.Tikhonov, Sechenov Institute of Evolutionary Physiology and Biochemistry of the Russian Academy of Sciences, 44 Thorez prospect, St. Petersburg 194223, Russia. Tel.: +007-812-552-3138; Fax: +007-812-552-3012; Email: tikhonov@vv3977.spb.edu. Dr. Zhorov's present address is Department of Biochemistry, McMaster University, Hamilton, Ontario, Canada. E-mail: zhorov@fhs.mcmaster.ca.

0006-3495/99/10/1914/13 $2.00

TABLE 1 Amino-acid sequences of M2 segments from several GluR subunits

	Relative Position in the M2																				
Subunit	1*	2	3	4*	5	6	7	8*	9	10	11*	12*	13	14	15	16*	17	18	19	20	21
NR1	L	T	L	S	S	A	M	W	F	S	W	G	V	L	L	**N**	S	G	I	G	E
NR2A	F	T	I	G	K	A	I	W	L	L	W	G	L	V	F	**N**	N	S	V	P	I
GluR1	F	G	I	F	N	S	L	W	F	S	L	G	A	F	M	**Q**	Q	G	C	–	D
GluR2	F	G	I	F	N	S	L	W	F	S	L	G	A	F	M	**R**	Q	G	C	–	D
NR1 (Cys)	C			C				C				C				C		C	C	C	
NR2 (Cys)								C					C			C	C	C	C	C	C

*Positions corresponding to the residues that face the pore in the present model. Residues affecting the PCP binding (Ferrer-Montiel et al., 1995) are underlined. The N/Q/R site residues are shown in bold. Positions of cysteine mutants that are labeled by sulfhydryl reagents in the NR1 and NR2A subunits (Kuner et al., 1996) are marked by C.

conductance, relative Ca^{2+} permeability, and blockade by polyamines decrease with the number of GluR2 subunits in the receptor oligomer (Blaschke et al., 1993; Brackley et al., 1993; Geiger et al., 1995; Burnashev et al., 1995; Swanson et al., 1996; Washburn et al., 1997). Homomeric receptors composed of the subunits with Arg residue at the N/Q/R site exhibit a very low conductance for cations and anions, as well as a low relative permeability for Ca^{2+} (Burnashev et al., 1996; Swanson et al., 1996, 1997). The low cationic permeability of the GluRs with Arg residues in the N/Q/R site may be due to the electrostatic repulsion of the permeating cations from the positively charged Arg. Table 2 lists the major properties of GluR channels that are controlled by the residues at the N/Q/R site.

Although the N/Q/R site is the major determinant of the channel permeability and blockade, other sites in the pore of GluRs also modulate these properties. For example, the block of AMPA channel by the intracellularly applied spermine is altered by the mutation of Asp residue at the C-end of M2 (Dingledine et al., 1992). The replacement of Leu^{577} in the GluR1 subunit by Trp (which is present in the homologous position of the NR1 subunit, see Table 1) increases Ca^{2+} permeability (Ferrer-Montiel et al., 1996). Ca^{2+} permeability of kainate channels depends on several residues in M1 and M2 (Kohler et al., 1993). Recent experiments provide evidence that different permeating properties of NMDA and AMPA receptors are determined by multiple sites (Wollmuth and Sakmann, 1998). Mutations of Trp^{607} in NR2A and NR2B subunits of NMDA receptor affect Mg^{2+} block and Ba^{2+} permeability (Williams et al., 1998).

The positively charged Arg in the N/Q/R site of GluR2 was suggested to control ion permeation properties in the heteromeric non-NMDA receptors (Burnashev et al., 1992a; Dingledine et al., 1992). However, it is difficult to explain substantially different properties (e.g., the pore diameter) of the channels having, in the N/Q/R site, Asn and Gln residues, which differ solely by the methylene group (Table 2). Assuming that the N/Q/R site forms the pore constriction, the longer Gln and Arg residues would be expected to protrude farther in the pore than the shorter Asn residues. However, experiments show that the pore of recombinant receptors with Asn in the N/Q/R site is significantly narrower than with Gln or Arg at this site (Villarroel et al., 1995; Burnashev et al., 1996). Furthermore, although the permeation of inorganic ions via GluR channels is expected to increase with the dimensions of the pore, NMDA channels with the smallest diameter are, in fact, the most permeable for monovalent (Swanson et al., 1996; Wyllie et al., 1996) and divalent cations (Mayer and Westbrook, 1987; Burnashev et al., 1995; Koh et al., 1995).

In the absence of experimental data on the three-dimensional structure of the N/Q/R site, the molecular mechanism that controls the channel properties at this site remains unknown. Under these circumstances, available experimental data may be used as restraints for molecular modeling of the N/Q/R site. An analysis of structure–activity relationships of various NMDA channel blockers (such as MK-801 and PCP-like compounds) have led Manallack et al. (1988) to propose a topographical model of the binding site for these blockers that incorporates an H-bond acceptor and a hydrophobic region. Wood et al. (1995) found a certain

TABLE 2 Properties of GluR channels governed by N/Q/R site

	Residue at the N/Q/R Site					
Property	Asparagine		Glutamine		Arginine	
Conductance (pS)	30–50	[ref. 1]	5–15	[ref. 2]	0.1–0.9	[ref. 2]
Ca^{2+} permeability (P_{ca}/P_{Na})	7–8	[ref. 3]	2–3	[ref. 3]	0.1	[ref. 4]
Pore diameter (Å)	5.5	[ref. 5]	7.5	[ref. 6]	7.5	[ref. 6]
Potent channel blockers	Variety		only few		none	

References: [1] Wyllie et al., 1996; [2] Swanson et al., 1996, 1997; [3] Koh et al., 1995, Mayer and Westbrook, 1987; [4] Geiger et al., 1995; [5] Villarroel et al., 1995; [6] Burnashev et al., 1996.

homology between M2s of GluRs and the pore loops in K^+ channels. Dingledine et al. (1992) proposed a salt bridge between the side chains of Arg^{16} in the N/Q/R site and Asp^{21} (see Table 1 for the residue numbering scheme used in this work). Sutcliffe et al. (1996) have built a molecular model of the non-NMDA receptor channels with M2s forming reentrant membrane loops. Williams et al. (1998) have proposed a schematic model with the conserved Trp^8 contributing (along with Asn^{16} residues) to the selectivity filter of NMDA channels. To the best of our knowledge, no atomic-scale models have been built to explain the role of the N/Q/R residues in NMDA and non-NMDA receptors.

In this work, we suggest that the residues in the N/Q/R site of GluRs do not completely extend in the pore: rather, their side chains form a macrocyclic structure stabilized by intersegment H-bonds. We have built several models of the macrocycles that explain, in a simple way, the apparent inconsistency between the nature of the residues in the N/Q/R site and the properties of the channels. Based on these models, we propose experiments that may help to test the underlying hypothesis on the intersegment H-bonds in the N/Q/R site.

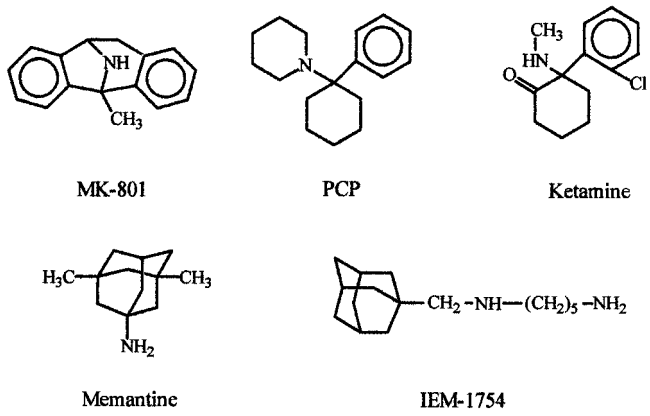

FIGURE 1 Potent blockers of the NMDA channel.

BACKGROUND OF THE MODEL

Our modeling study is based on the assumption that the ionotropic NMDA and non-NMDA receptors have a similar arrangement of the pore-lining M2s. This assumption is supported by the following observations. First, in NMDA and non-NMDA GluRs, the channel-forming M2s do not span the membrane but form reentrant membrane loops (Wo and Oswald, 1994; Hollmann et al., 1994; Bennett and Dingledine, 1995; Kuner et al., 1996). Second, in all GluRs, residues at the N/Q/R site that control the channel properties are located at homologous positions (see Table 1). Third, certain channel properties presumably associated with particular residues in the N/Q/R site may be predictably engineered by the site-directed mutations at the N/Q/R site.

Gln has a longer side chain than Asn. At first sight, Gln residues are expected to protrude farther into the pore and make the AMPA channel narrower than the NMDA channel. However, AMPA channels permeate larger organic cations than NMDA channels (Villarroel et al., 1995; Burnashev et al., 1996). In spite of the larger dimensions, AMPA channels are less permeable for inorganic cations than NMDA channels (Burnashev et al., 1995; Wyllie et al., 1996; Swanson et al., 1996, 1997) suggesting different structures of the selectivity filters in these two channels.

Potent organic blockers of NMDA channel have a protonated amino group (see Fig. 1), which is thought to form an H-bond with a proton acceptor group in the channel (Manallack et al., 1988). The replacement of the residues in the N/Q/R site of GluRs affects the binding of the blockers (Mori et al., 1992; Ferrer-Montiel et al., 1995; see Table 2) suggesting that the N/Q/R site incorporates proton acceptors. Surprisingly, whereas the H-bonding properties of Asn and Gln residues are similar, many compounds that block the NMDA channel are not active on non-NMDA channels with Gln at the N/Q/R site (Ruppersberg et al., 1993; Ferrer-Montiel et al., 1998). This suggests that, in the non-NMDA channels, the Gln side-chain oxygens do not accept H-bonds from the ligands in the pore. Thus, the results of pharmacological and electrophysiological experiments are inconsistent with the idea that the residues in the N/Q/R site freely extend into the pore.

We propose that the residues in the N/Q/R site form a cyclic structure stabilized by intersegment H-bonds. The cyclic structures of the N/Q/R site provide a simple explanation for the seemingly paradoxical experimental data. First, the longer side chains of Gln residues would form the larger cycle, i.e., the wider pore constriction at the N/Q/R site as compared with the ring of Asn residues. Second, intersegment H-bonds would significantly restrain the conformational freedom of the N/Q/R site residues. The smaller ring formed by the Asn residues may have optimal conformations with the side chain oxygens protruding into the pore and accepting H-bonds from the blockers, whereas, in the larger cycle formed by the Gln residues, these oxygens may be inaccessible from the pore. In such a case, the narrower NMDA channel would display a higher permeability for the hydrated inorganic cations than the wider AMPA channel in which the pore-exposed CH_2 groups of the Gln residues would obstruct the permeation.

The smallest ring of the N/Q/R residues could have the Asn/Gln side chain in a given subunit H-bonded to the side chain of the homologous residue in the adjacent subunit. However, the rings involving side-chain-to-side-chain H-bonds are unlikely because of two reasons. First, Asn and Gln residues would form similar side-chain-to-side-chain rings that would not explain the essential differences in properties of the corresponding channels. Second, the side chain of the protonated Arg lacks H-bond acceptors and, hence, cannot be involved in a cyclic structure with side-chain-to-side-chain H-bonds. This leaves the side-chain-to-main-chain H-bonds as possible candidates to stabilize the cyclic structures of the N/Q/R site. The simplest model

would have the side-chain NH_2 group donating the H-bond to the main-chain oxygen of the homologous residue in the adjacent subunit (Fig. 2).

METHODS

The Monte Carlo minimization (MCM) protocol (Li and Scheraga, 1988) and the ECEPP/2 force field (Momany et al., 1975; Nemethy et al., 1983) were used for searching the optimal conformations in the space of generalized coordinates. Bond lengths and angles were assigned the standard values that were kept rigid in energy minimizations. Calculations were carried out on a Pentium II PC using the ZMM package (Zhorov, 1981). Atom–atom interactions were calculated with a cutoff distance of 8.0 Å. MCM trajectories were calculated at $T = 600$ K. Trajectories were terminated when the last 500 energy minimizations did not lower the energy of the lowest minimum-energy conformation (MEC) found. Hydrogen bonds were imposed using the flat-bottom distance restraints of 1.7–2.2 Å. For the subsequent analysis, we selected the MECs with the energies up to 7 kcal/M from the apparent global minimum found in the trajectory. These structures were subsequently minimized without restraints at the N/Q/R site. Other details of the calculations are described elsewhere (Zhorov and Ananthanarayanan, 1996). Assembling of the models, and their visualization and rotation were performed using molecular visualization and manipulation, an MS DOS program for IBM PC (D. B. Tikhonov, unpublished) that provides an interactive interface for the ZMM package. Because of dynamic memory allocation, the number of atoms is limited only by the computer memory. The objects are visualized in 256 colors with a screen resolution up to 1024/768 pixels using a Z-buffer. As in the case of MOLMOL program (Koradi et al., 1996), the molecular visualization and manipulation allows translations and rotations of individual molecules in multimolecular complexes, thus providing the possibility of assembling complex structures.

In this work, we use the numbering scheme by which the N/Q/R site corresponds to position 16 in M2 (see Table 1). The N/Q/R site of GluRs has Asn, Gln, or Arg residues that may form a ring stabilized by the intersegment H-bonds with the side chains oriented in the clockwise or counterclockwise direction. The stoichiometry of GluRs remains unclear. Some data are consistent with a pentameric organization (Wenthold et al., 1992; Ferrer-Montiel and Montal, 1996), while increasing evidence suggests a tetrameric organization (Wood et al., 1995; Wu et al., 1996; Laube et al., 1998; Mano and Teichberg, 1998; Rosenmund et al., 1998). In this work, we build and analyze twelve homooligomeric models with different residues at the N/Q/R site, different numbers of subunits in the receptor oligomer, and different direction of the cycle closing. A three-letter code is used to designate a specific model. For example, Q4c designates the model with Gln residues at the N/Q/R site (the symbol Q), the tetrameric stoichiometry (the symbol 4), and the clockwise direction of the vectors drawn from C^{α} to N^{ϵ} of each Gln residue in the extracellular view of the channel (the symbol c).

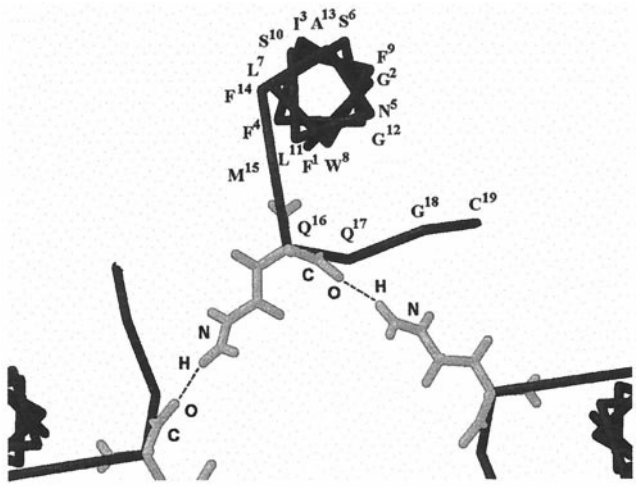

FIGURE 2 A proposed system of the intersegment H-bonds closed in the clockwise direction viewed from the outside of the cell. M2 of one subunit and parts of the adjacent M2s are shown as C^{α}-tracing. Gln^{16} residues of the N/Q/R site are shown as sticks. NH_2 group of Gln^{16} in a given M2 segment and the main-chain C═O group in the adjacent M2 segment form an H-bond. M2 helices are disordered at the N/Q/R site, the N/Q/R residues protrude in the pore, whereas the C-ends of M2s turn out of the pore.

It is known that residues beyond the N/Q/R site in M2s also affect ion-permeating and ligand-binding properties of GluRs. The present model is focused on the N/Q/R site structure. We assume for simplicity that the structure of M2s does not significantly affect the H-bonding pattern at the N/Q/R site. Our calculations support this assumption (see Results and Discussion). GluR1 can form homomeric receptors and, therefore, is a good candidate for homomeric models of GluRs. For the sake of simplicity, all models are built with M2 from the GluR1 subunit (positions from 1 to 19) except positions 16 and 17 in which N, Q, and R models have, respectively, Asn-Ser (NS), Gln-Gln (QQ), and Arg-Gln (RQ) dipeptides (see Table 1).

Each model was initially assembled as a symmetrical bundle of M2s. The optimal structures of individual M2s were MC-minimized from the starting α-helical geometry with the constrained α-helical H-bonds. In all the models, the residues in positions 1, 4, 8, 11, and 12 were oriented to face the pore (see Fig. 2), as shown by the cysteine-scanning analysis of NMDA receptor (Kuner et al., 1996). In the absence of experimental data on the angle between the membrane plane and the axes of M2s, the latter were oriented parallel to the pore axis. Taking into account the maximal diameter of GluR channels (8.8 Å) as estimated by Wollmuth et al. (1996) and dimensions of the residues in the pore-facing positions 1, 4, 8, 11, and 12, the distance between the pore axis and the M2 axes was chosen to be 11.5 Å.

The N-ends of M2s (positions 1–13) were fixed in the α-helical conformation. A given disposition of the helical axes was restrained by fixing the backbone geometry as well as the Cartesian coordinates and Euler angles of the root atom in each M2. All torsions in residues 14–19 were randomized in the MCM protocol and varied during energy minimizations. Although conformations with the side-chain oxygens from several residues protruding into the pore at the same level are electrostatically unfavorable, permeating cations may stabilize them. We simulated this possibility by inserting Na^+ in the center of the pore at the level of N/Q/R site in the N- and Q-models.

RESULTS AND DISCUSSION

Geometry of the N/Q/R rings

The starting structures for the MCM trajectories were assembled from the entirely α-helical M2s with restraints imposing intersegment H-bonds in the N/Q/R site. As was expected, the above restraints conflicted with both the four-helical- and the five-helical-bundle topologies. The trajectories yielded structures (see Fig. 3) in which M2 helices were disordered at the level of N/Q/R site, with the N/Q/R residues protruding in the pore and the C-ends of M2s turning out of the pore. Parameters of the MCM trajectories and characteristics of the structures obtained are given in Table 3. Analysis of the voltage-dependent block of NMDA channel by externally and internally applied drugs suggests that, unlike the funnel-shaped channel in the nicotinic acetylcholine receptor (Galzi and Changeux, 1995), NMDA channel has wide inner and outer vestibules and a thin

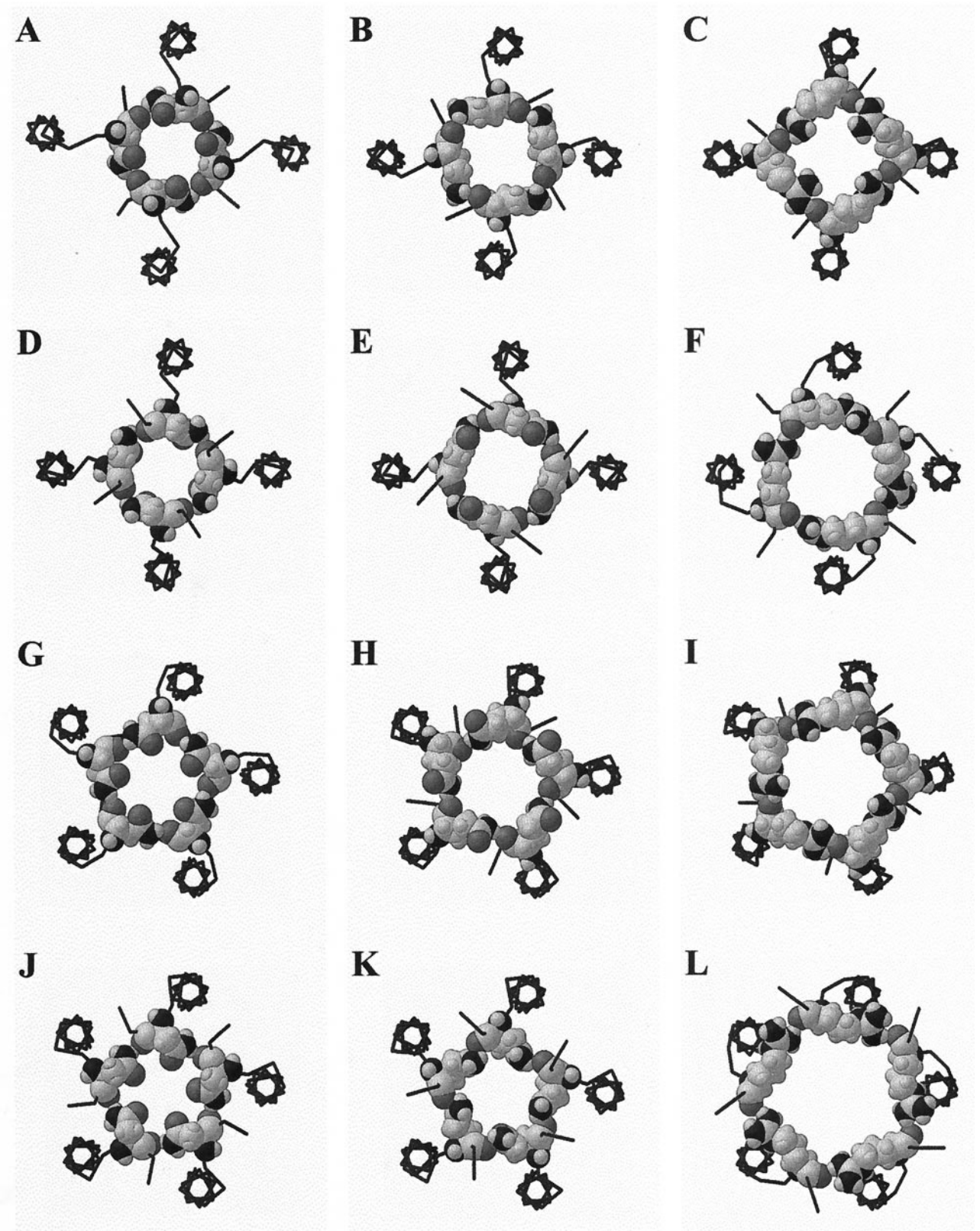

FIGURE 3 Extracellular view of the representative conformers of the N/Q/R site models. N/Q/R site residues are space filling, remaining portions of the M2s are shown as C^{α}-tracings. Nitrogen, oxygen, and carbon/hydrogen atoms are shown in black, gray, and light-gray, respectively. The cyclic structures of the N/Q/R site are stabilized by the intersegment H-bonds. (*A–L*) Respectively, designate the models N4a, Q4a, R4a, N4c, Q4c, R4c, N5a, Q5a, R5a, N5c, Q5c, and R5c.

TABLE 3 Models of the N/Q/R site

Model	N steps*	MECs[#]	Conf[§]	D[¶]	O—Dir[‖]
N4a	8300	57	21	5.6	in
N5a	9100	45	11	6.0	in
Q4a	7100	49	18	6.9	out
Q5a	12800	43	23	7.0	out
R4a	8400	53	22	7.2	–
R5a	7200	49	26	8.0	–
N4c	7600	57	41	5.8	in/out
N5c	14300	38	18	6.9	in
Q4c	6600	50	23	7.3	in/out
Q5c	8800	52	27	8.3	out
R4c	7900	78	33	8.0	–
R5c	8800	64	27	9.7	–

*The number of energy minimizations during the MCM search.
[#]The number of MECs obtained.
[§]The number of low-energy M2 conformers.
[¶]The average cycle diameter (Å).
[‖]The preferable orientation of Asn (Gln) side-chain oxygens (in, inside the pore; out, outside the pore).

narrow selectivity filter (Zarei and Dani, 1995). In our models, the pore of GluRs is wide with the exception of the N/Q/R site constriction stabilized by the intersegment H-bonds. The model agrees with the fact that the replacement of Asn by Gly in NMDA receptor increased the effective channel diameter from 5.5 to 8.8 Å (Wollmuth et al., 1996). Because Gly residues cannot be involved in the proposed system of cyclic H-bonds, the Gly-containing pore should be wider.

The MCM search yielded several types of H-bonds that were not imposed by the restraints (see Table 4). Moreover, these H-bonds stabilize optimal conformations of the N/Q/R site. For example, main-chain-to-main-chain H-bonds involving residues in positions 15 and 17 (type 1) stabilize the cyclic structure of the N/Q/R site in the counterclockwise models, whereas the H-bond of type 2 stabilizes the clockwise models. The involvement of the residue at position 17 in the H-bond network is of special interest. GluR subunits have Ser, Asn, or Gln at this position (Table 1). At the helix termination near the N/Q/R site, several polar main-chain groups are disengaged from the network of the α-helical H-bonds. The polar side chain of the residue in position 17 may form H-bonds with some of the groups disengaged from the α-helical H-bonds (e.g., type 3, type 5, and type 6 H-bonds). This may explain why mutation of Gln^{17} to Ser^{17} in GluR1 yields inactive receptors (Ferrer-Montiel et al., 1995). In heteromeric NMDA receptors, Asn^{17} of the NR2 subunit affects the channel properties more strongly than Asn^{16} (Wollmuth et al., 1996, 1998). A possible explanation is that, in the NR2 subunit, Asn^{17} rather than Asn^{16} is involved in the cyclic system of H-bonds. The fact that M2s of the NR1 and NR2 subunits differ in their secondary structure (Kuner et al., 1996; Kashiwagi et al., 1997) is consistent with this idea.

TABLE 4 Additional H-bonds found in the MCM calculations

Type	H-bond	Models
1	Met^{15}–O· · ·H–Ser^{17}	N4a, N5a
	Met^{15}–O· · ·H–Gln^{17}	Q5a, R5a, Q4a
2	Met^{15}–H· · ·O–Gly^{18}	N5c, Q5c, Q4c
3	Leu^{11}–O· · ·H^{γ}–Ser^{17}	N5a
4	Met^{15}–O· · ·H^{δ}–Asn^{16}	N5c
5	Met^{15}–O· · ·H^{γ}–Ser^{17}	N4a, N5a
6	Gln^{16}–O^{δ}· · ·H^{ε}–Gln^{17}	Q5a, Q4a
7	Asn^{16}–H^{δ}· · ·O–Ser^{17}*	N4c, N5c
8	Gln^{17}–O· · ·H^{η}–Arg^{16} [#]	R5a
9	Phe^{14}–O· · ·H–Arg^{16}	R4c, R5c
10	Phe^{14}–O· · ·H–Gln^{17}	R5
11	Met^{15}–O· · ·H–Cys^{19}	N4c
12	Asn^{16}–H^{δ}· · ·O–Ser^{17} [#]	N4c
13	Cys^{19}–O· · ·H^{δ}–Asn^{16}	N4c

*Residue belongs to the adjacent segment located counterclockwise to the given segment.
[#]Residue belongs to the adjacent segment located clockwise to the given segment.

The cysteine scanning analysis showed accessibility of C-ends of M2s for sulfhydryl reagents (Kuner et al., 1996). The tetrameric but not the pentameric models have sufficient space between the helical portions of M2s to accommodate the extended C-ends. However, this fact cannot be used as an argument against the pentameric models built with the fixed disposition of the helical portions in positions 1–13. To some extent, the H-bonding patterns of the N/Q/R rings are insensitive to the angle between the helices. In real channels, the cytoplasmic portion may be wider than in our models, and the helical segments of M2s may diverge to allow C-ends to penetrate between the helices and contribute to the pore.

The optimal models obtained vary in the dimensions of the N/Q/R ring and in the chemical nature of the groups forming the pore narrowing. In the pentameric models, the average diameter of the pore increases from N-models to R-models and exceeds the experimental diameters of the corresponding recombinant GluR channels (Tables 2 and 3). The optimal conformations of preliminary tetrameric models had the average diameters of the pore smaller than those observed experimentally. To test whether the tetrameric models have MECs matching the experimental dimensions of the pore, we have imposed additional distance restraints between the side-chain nitrogens of the adjacent N/Q/R residues. These N–N restraints exclude conformers with small diameters of the pore, thus simulating possible pore-stretching interactions that are ignored in our model. Various distances were tested for the N–N restraints. In N4 models, the maximum distance of the N–N restraint not conflicting with the cycle-closing restraints is 8.3 Å. In Q4 models, the maximum distance of the N–N restraint is 9.5 Å. In tetrameric models, the average diameters of the cycles obtained with the N–N restraints are in good agreement with experimental results (see Table 3). Thus, both tetrameric and pentameric models explain the fact that Gln and Arg residues in the N/Q/R site form a wider pore constriction than does the Asn residue. The pore dimensions with the N–N restraints are in better agreement with experiments for tetrameric models than for pentameric models.

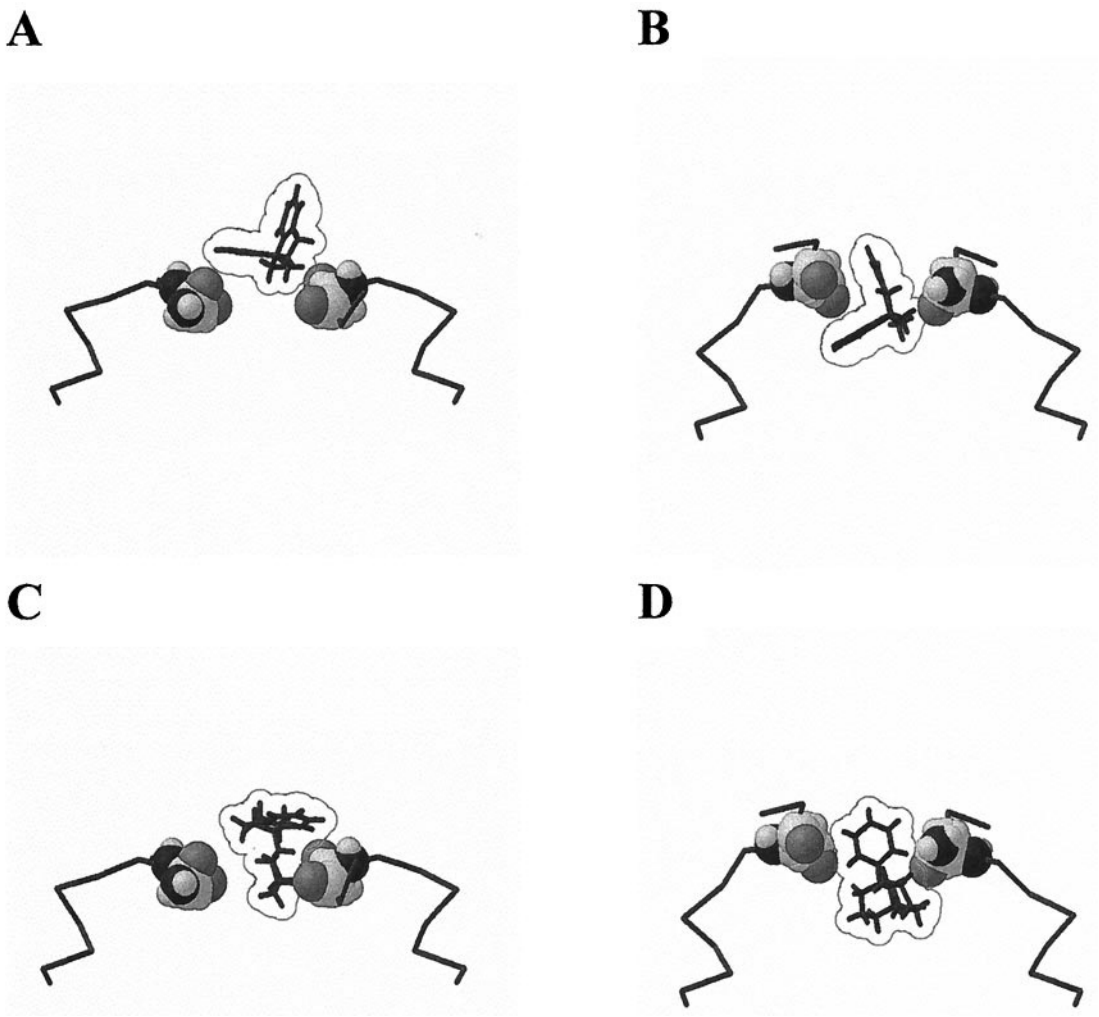

FIGURE 4 Side views at the (*A*, *C*) N4a and (*B*, *D*) N4c models forming energetically optimal complexes with (*A*, *B*) MK-801 and (*C*, *D*) phencyclidine. Only two nonadjacent M2 segments are shown. Asn residues of the N/Q/R site are space filling whereas the blockers are shown as sticks with van der Waals contours. The ammonium groups of the blockers form H-bonds with Asn side-chain oxygen. Different binding modes of the same blocker are due to the different orientation of the Asn side-chain oxygens in the clockwise and counterclockwise models.

At the present stage of the study, it is difficult to determine all possible H-bonding systems and select the most preferable one. The models comprise only 19 residues in each M2 and neglect interactions with other parts of the receptor. The models also ignore intrapore water molecules that may contribute to the stability of different structures (Sankararamakrishnan and Sansom, 1995). We have demonstrated the possibility of various cyclic structures and roughly estimated their relative stability. In real channels, the N/Q/R site may adopt a preferable cyclic conformation or may exist as an equilibrium of several conformations. Both clockwise and counterclockwise models yield conformers with similar properties. Further studies are necessary to favor one of the models.

Blockers and Ca^{2+} in the pore

In the majority of the optimal conformers of the models N5c, N5a, Q4c, and N4a, the pore constriction is lined by the side-chain oxygens of Asn^{16} or Gln^{16}. In contrast, only in a few conformations of the models Q5c, Q5a, and Q4a, do the side-chain oxygens of Gln^{16} face the pore. The orientation of Asn side-chain oxygens in the pore may explain the high permeability of NMDA channels and their block by organic compounds. Studies of the structure–activity relationships of the NMDA channel blockers yielded topographic models of their binding site (Manallack et al., 1988; Lyle et al., 1990). All NMDA receptors are heterooligomers, with conformations of M2s in NR1 and NR2 subunits being essentially different (Kuner et al., 1996; Wollmuth et al., 1996, 1998). Our homomeric N-models comprise M2s that may be considered as a double mutant of GluR1 (Gln^{16} to Asn^{16} and Gln^{17} to Ser^{17}). This simple model is not expected to explain completely the structure–activity relationships of the NMDA channel blockers. In addition, because only a few blockers of non-NMDA channels are known, a comprehensive analysis of their structure–activity relationships would be premature. Nevertheless, we

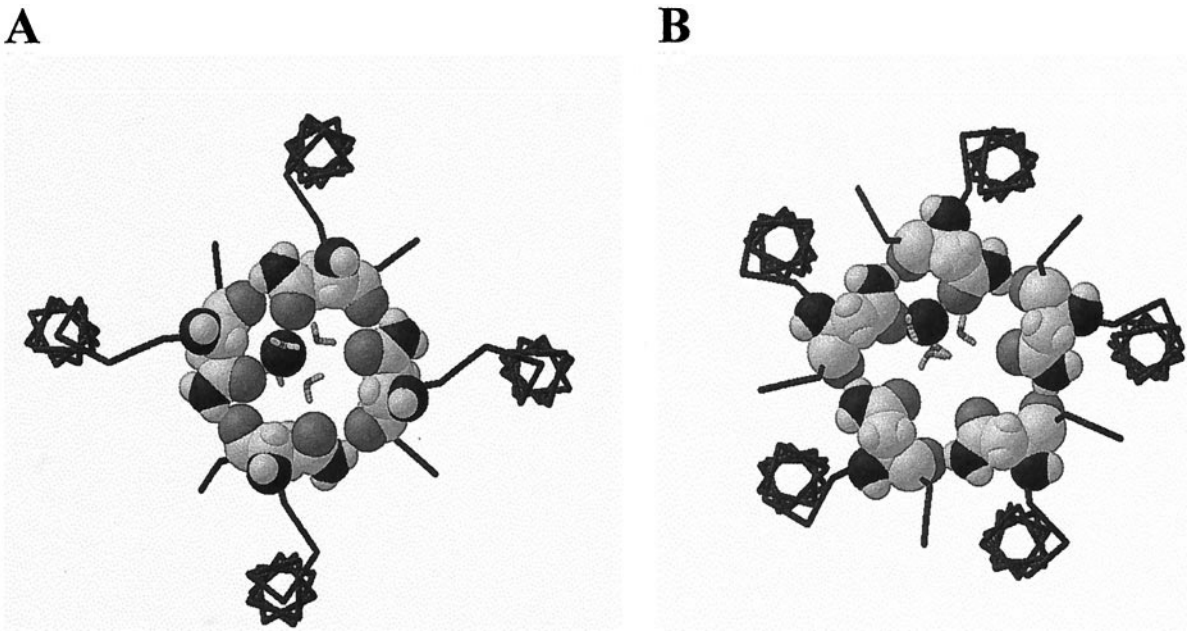

FIGURE 5 Possible interactions of Ca^{2+} with the N/Q/R site in NMDA channels. The models (*A*) N4a and (*B*) N5a are viewed from the extracellular side with the space-filling Asn residues. Ca^{2+} ion is shown as a black sphere inside the pore, and waters of the inner hydration shell of Ca^{2+} are shown as sticks. Ca^{2+} interacts with two Asn side-chain oxygens that substitute two water molecules of the hydration shell. The tetrameric model perfectly fits the partially dehydrated Ca^{2+}, whereas Asn side-chain oxygens either coordinate Ca^{2+} or accept H-bonds from the hydration shell. In the pentameric model, one Asn residue does not interact with Ca^{2+} nor with the inner hydration shell; the empty space could be filled by a water molecule from the second hydration shell of Ca^{2+} (not shown).

attempted to visualize possible binding modes of the channel blockers by performing the MCM docking of MK-801 and PCP (Fig. 1) in representative structures of the N-models. The H-bond between the blocker's amino group and Asn side-chain oxygen was imposed using a distance restraint of 1.7–2.0 Å, while the backbones of M2s were kept rigid. The optimal binding modes found are shown in Fig. 4.

In the clockwise models, the bonds C^{γ}—O^{δ} of Asn^{16} point to the cytoplasm, whereas, in the counterclockwise models, they point in the extracellular direction, being collinear with the α-helical dipole moment. N4c and N4a models suggest different binding modes for MK-801 and for PCP (Fig. 4). To reach the binding site in the N4c model, bulky groups of the blockers should pass the N/Q/R narrowing. In the optimal binding mode in both N4c and N4a models, the second aromatic group of PCP passes the channel narrowing, approaching Leu^{11}, which is located one helical turn closer to the cytoplasm than is the N/Q/R site. The replacement of Leu^{11} in the GluR1 receptor by Trp (note Trp^{11} in NMDA receptor subunits, see Table 1) increases the blocking potency of PCP without affecting the channel block by MK-801 (Ferrer-Montiel et al., 1995). Our modeling shows that MK-801 is too short to interact simultaneously with the N/Q/R site and Trp^{11}.

Dicationic compounds with an adamantane group, e.g., IEM-1754 (Fig. 1) were demonstrated to block effectively open channels in both NMDA and GluR2-lacking AMPA receptors (Antonov et al., 1995; Magazanik et al., 1997). The adamantane group itself does not determine the anti-AMPA activity because memantine, a monocationic adamantane derivative, blocks NMDA but not AMPA channels. The high activity of IEM-1754 in blocking the AMPA channel is apparently due to the presence of the second ammonium group that could interact with an ancillary nucleophilic site. Such a site may be formed by Trp^{8}, which is highly conserved in all subunits of GluRs and affects binding of polyamines (Kashiwagi et al., 1997; Williams et al., 1998). The hydrophobic adamantane moiety could bind to Gln^{16} residues, whereas the distant amino group would pass the N/Q/R ring to reach the deeper ring of Trp^{8} residues. Amino–aromatic interactions may stabilize such binding as in the case of interaction between acetylcholine and acetylcholinesterase (Sussman et al., 1993). An ancillary nucleophilic site may also be formed by Asp^{21} located at the carboxyl end of M2s (near the cytoplasm). Indeed, the replacement of Asp^{21} to Asn affects the blocking potency of the internally applied polyamines (Dingledine et al., 1992; Washburn and Dingledine, 1996). Thus, our models suggest that Asn residues in the N/Q/R site of NMDA channel form a nucleophilic site for various cationic blockers, whereas the side-chain oxygens in the homologous Gln residues of AMPA channels are inaccessible for H-bond donors in the blocking molecule. Therefore, blockers of these channels should interact with an ancillary nucleophilic site.

The channels with Asn and Gln residues at the N/Q/R site have different ion-permeation properties. Our models qualitatively explain the fast permeation of inorganic cations, in

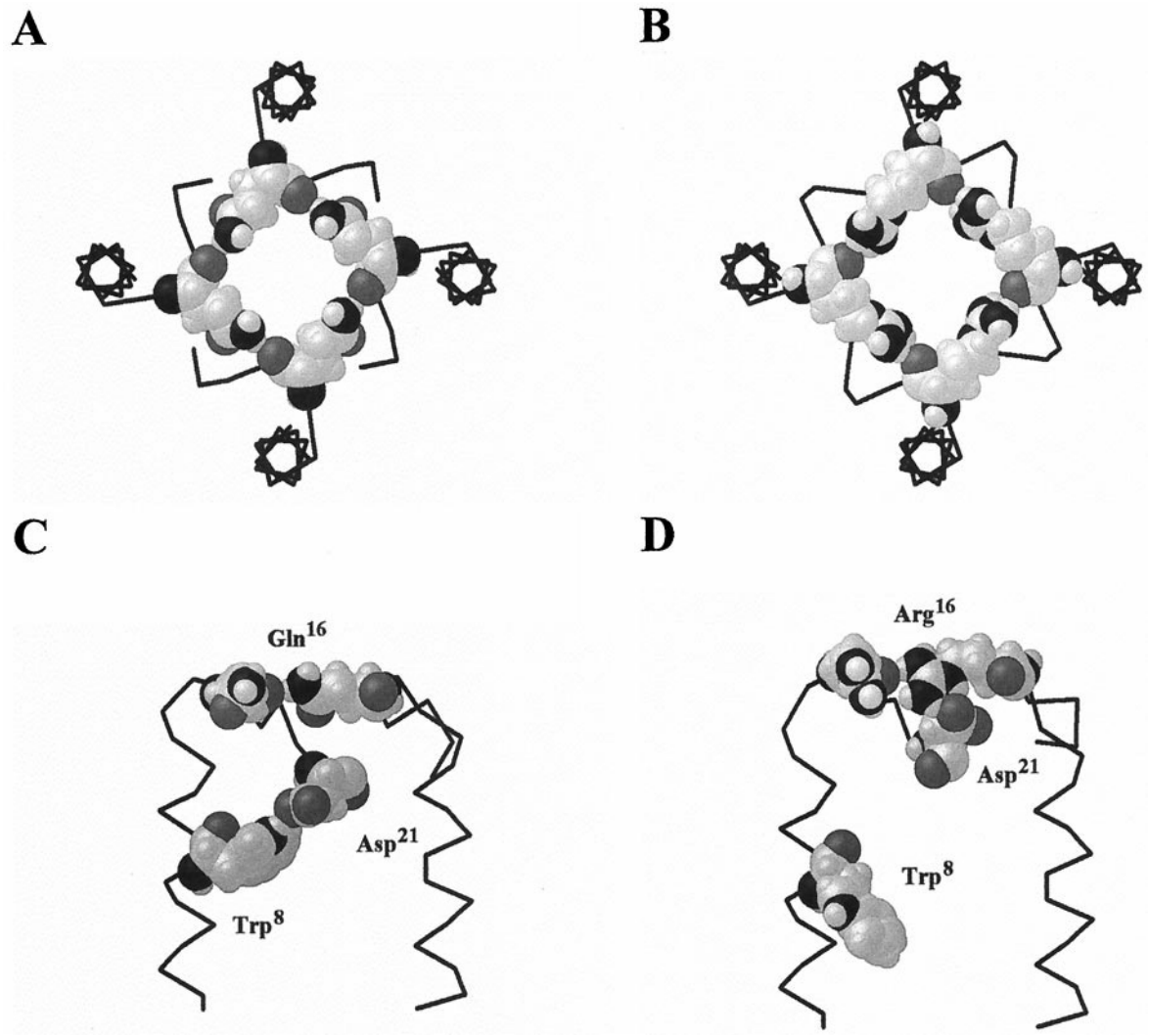

FIGURE 6 Extended models (*A*, *C*) Q4a-D and (*B*, *D*) R4a-D viewed (*A*, *B*) from extracellular side and (*C*, *D*) from the membrane exposed side with only two adjacent segments shown. N/Q/R site residues and residues at positions 8 and 21 (in *C* and *D*) are space filling, and the remaining portions of M2s are shown as C^{α}-tracing. In the Q4a-D model, Asp^{21} interacts with Trp^{8} forming an additional nucleophilic site exposed to the pore. In the R4a-D model, Asp^{21} binds to Arg^{16} from the adjacent M2 segment and screens the positive charge of Arg^{16}, thus allowing cations to pass through.

particular Ca^{2+}, through NMDA channels by exchange of water(s) in the cation hydration shell for the O^{δ} of Asn. The inner hydration shell of Ca^{2+} comprises at least six water molecules. The pore constriction in the NMDA receptor is as small as 5.5 Å in diameter. It can accommodate the cation with only two waters in the plane normal to the pore axis. Two waters of the inner hydration shell may extend above and below the plane. To test whether the remaining two waters from the Ca^{2+} inner hydration shell may be substituted by the channel oxygens, we have imposed two distance restraints between Ca^{2+} and Asn O^{δ} atoms in the adjacent segments and four distance restraints between Ca^{2+} and water molecules. The representative structures for pentameric and tetrameric models found in the MCM trajectories are shown at Fig. 5. The tetrameric model fits Ca^{2+} with the four waters, two of which form H-bonds with the side-chain oxygens not involved in the restraints. The pentameric model also accommodates hydrated Ca^{2+}, but one Asn does not interact with Ca^{2+} or its inner hydration shell; the empty space left in the plane of the N/Q/R ring could be filled by a water molecule from the second hydration shell of Ca^{2+}.

Possible interaction of C-end aspartates with Arg in the N/Q/R site

Arg residues in the N/Q/R site of GluRs diminish the permeation of inorganic cations (Geiger et al., 1995; Swanson et al., 1996, 1997) and the binding of cationic blockers (Herlitze et al., 1993; Magazanik et al., 1997; Washburn et al., 1997). This effect may be due to the electrostatic repulsion of the cations from the positively charged Arg residues. Our R-models show Arg residues at the N/Q/R site forming

the H-bonded ring with the Arg side chains protruding in the pore. This would reduce the cationic permeability and increase the anionic one, in agreement with experimental observations (Geiger et al., 1995; Swanson et al., 1996, 1997). Homomeric channels with Arg residues at N/Q/R site are permeable for both cations and anions (Burnashev et al., 1996). However, the mechanism by which cations pass a ring of Arg residues remains unclear. Some factors not considered in the models described above could partially screen the electrostatic effect of the Arg ring. GluR subunits have a negatively charged Asp^{21} at the C-end of M2 (see Table 1). Dingledine et al. (1992) and Sutcliffe et al. (1996) proposed a coupling of Asp^{21} with Arg^{16} (N/Q/R site) to explain the cationic permeability of the Arg-containing GluRs. To test whether our models agree with this idea, we have performed additional calculations of the Q4a-D and R4a-D models that were obtained from the Q4a and R4a models by extending their M2s up to Asp^{21} (D).

The MCM calculations of the Q4a-D model show that Asp^{21} at the movable C-end of M2 may approach several residues. The interaction of Asp^{21} with the side-chain NH group of Thr^{8} (Fig. 6 *C*), the residue conserved in GluR subunits, is of special interest because a similar motif is seen in the x-ray structure of the KcsA K^+ channel (Doyle et al., 1998; see Concluding Remarks). Mutations of both Asp^{21} and Trp^{8} affect the channel properties (Dingledine et al., 1992; Kashiwagi et al., 1997). In the conformations with the $O^{\delta}\cdots H^{\epsilon}$ H-bond involving Asp^{21} and Trp^{8}, the side-chain carboxyl oxygens of Asp^{21} face the pore, forming a nucleophilic ring that may be important for permeation properties of GluR channels and for the binding of dicationic blockers (Fig. 7).

In the R4a-D model, electrostatic interactions stabilize conformations with Asp^{21}-Arg^{16} salt bridges and $O^{\delta}\cdots H^{\epsilon}$ intersegment H-bonds between Asp^{21} and Arg^{16} (Fig. 6 *D*). Because Arg side chain can donate several H-bonds simultaneously, interactions between Arg^{16} and Asp^{21} do not significantly affect the geometry of the N/Q/R ring stabilized by the intersegment H-bonds involving Arg^{16} residues (Fig. 6, *A* and *B*).

Superposition of the Q4a-D and R4a-D models shows homologous Asp^{21} C^{α} atoms separated by only 3.5 Å. Therefore, only a small shift of the C-end would enable Asp^{21} to approach either Trp^{8} or Arg^{16}. Comparison of the Q4a-D and R4a-D models (Fig. 6) suggests that Arg^{16} may affect the channel properties by screening the nucleophilic effect of the Asp^{21} side-chain oxygens. Thus, our models explain the permeability of the channels with an Arg ring, in agreement with previous suggestions (Dingledine et al., 1992; Sutcliffe et al., 1996; Washburn and Dingledine, 1996).

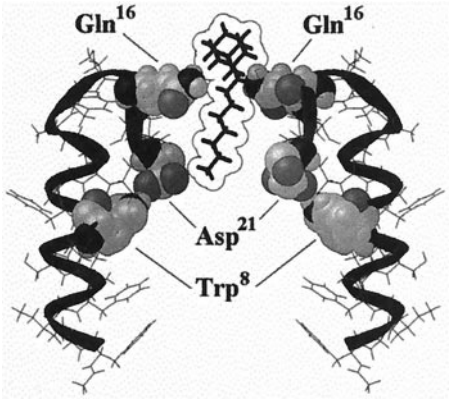

FIGURE 7 A possible binding mode of IEM-1754, the AMPA channel blocker, in the Q4a-D model. Side view with only two nonadjacent M2s shown. Trp^{8}, Gln^{16}, and Asp^{21} residues are space filled, and the remaining portions of M2s are shown as a ribbon. The blocker is shown as sticks with van der Waals contours. The adamantane group of the blocker binds to the ring of Gln^{16} residues in the N/Q/R site, whereas the distant ammonium group penetrates deeper to interact with Asp^{21}.

CONCLUDING REMARKS

In this work, we have proposed a cyclic motif of the N/Q/R site stabilized by intersegment H-bonds. The optimal structures of the site found by the MCM search helped us to explain such seemingly paradoxical experimental data as the lack of correlation between the dimensions of the channel and the size of the pore-facing residues, the lack of correlation between the channel permeability for organic and inorganic cations, and different pharmacological properties of NMDA and non-NMDA channels (Table 2). The proposed models may help design new experiments. For example, models were proposed in which dicationic compounds interact with two nucleophilic sites in nAChR channel (Brovtsyna et al., 1996; Tikhonov and Zhorov, 1998). Some dicationic compounds also block non-NMDA channels (Magazanik et al., 1997) suggesting that they may be used to probe the ligand-binding-site topography of GluRs and their mutants. In view of our models, the primary targets for the combined mutational and ligand-binding studies are positions 8, 11, and 21 that affect ion permeability and pharmacological sensitivity of GluRs. The distance between the N/Q/R site and ancillary nucleophilic site estimated from such studies may provide important information for further modeling of GluR channels. Because AMPA and kainate subunits can form homomeric receptors, they seem to be the most attractive objects for combined mutagenesis, ligand binding, and molecular modeling studies.

The tetrameric model with the N/Q/R ring closed in the counterclockwise way is more consistent with the available experimental data than other models, which, however, cannot be ruled out. Further modeling studies may specify the H-bonding network and locate additional groups involved in the binding of dicationic blockers.

Functionally, GluRs resemble nicotinic acetylcholine receptors: both mediate transmission at fast chemical synapses and form low-selectivity cationic channels. However, the structure of GluR channels differs markedly from that of acetylcholine receptor. The pore-forming M2s in GluRs do not span the membrane but form a reentrant membrane loop.

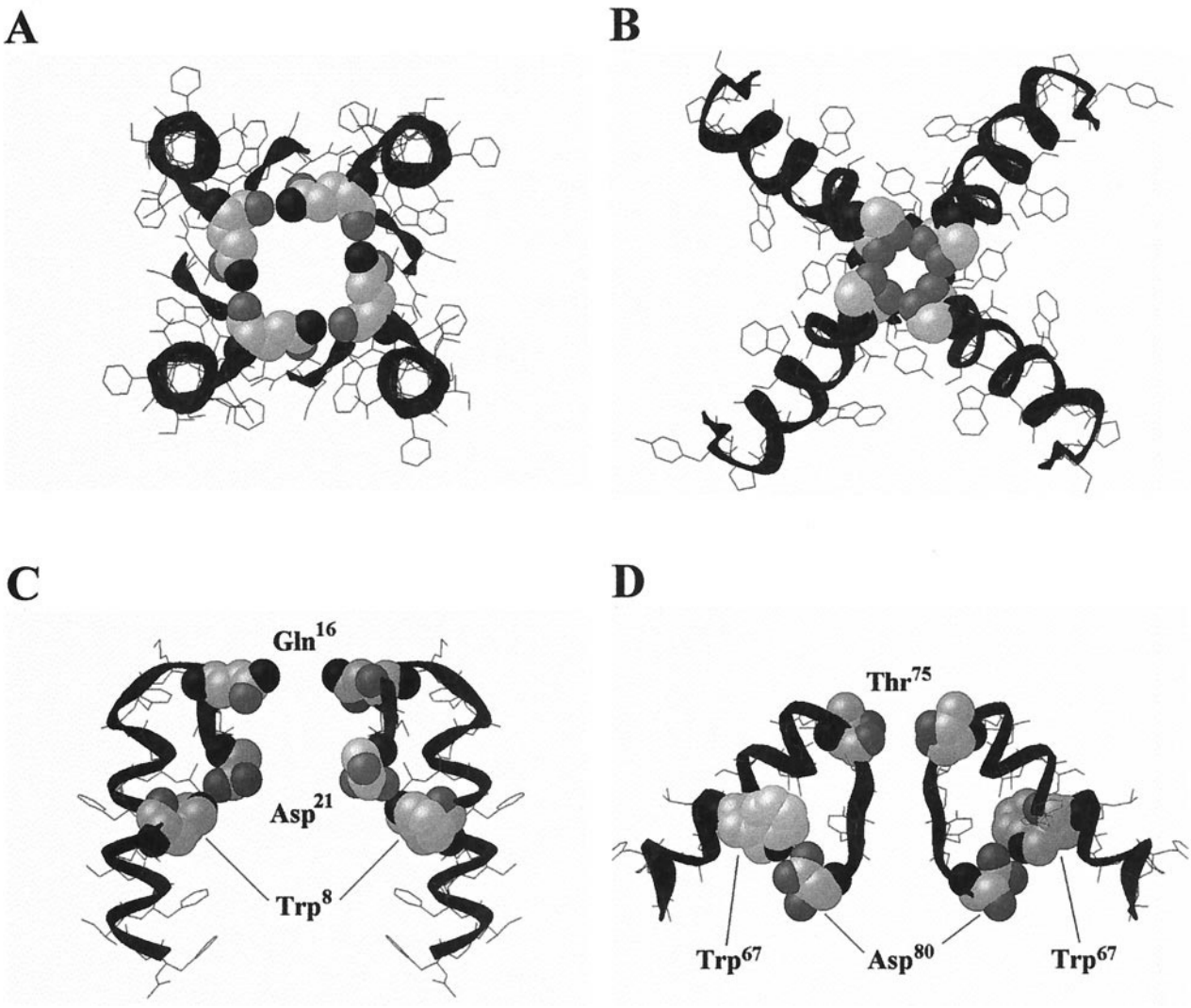

FIGURE 8 (*A*, *C*) Q4a-D model and the (*B*, *D*) x-ray structure of the KcsA K^+ channel viewed from (*A*) the extracellular, (*B*) intracellular, and (*C*, *D*) the membrane-exposed sides with only two nonadjacent segments shown. The GluR residues at positions 8, 16, and 21 and the homologous residues in the KcsA K^+ channel are space filling, and the remaining portions of M2s are shown as ribbons. In both channels, the pore constrictions are formed by the rings of hydrophilic residues stabilized by the intersegment H-bonds with the side-chain oxygens exposed to the pore. In both channels, the Asp residue at the C-end of the pore-lining segment is H-bonded to the Trp in the N-end half of the segment.

In this respect, GluRs resemble voltage-gated K^+ channels. Indeed, M2s of GluRs are homologous with the pore-forming domains in K^+ channels, whereas the homology with acetylcholine receptor channel is poor (Wood et al., 1995).

The x-ray structure of the K^+ channel from *Streptomyces lividans* (KcsA K^+ channel; Doyle et al., 1998) shows the membrane reentrant loops at the pore region with four α-helices terminated near Thr^{75}, the position homologous to the N/Q/R site in GluRs. Kuner et al. (1996) have proposed a similar structure for an M2 reentrant loop of the NMDA receptor with the helices terminated near the selectivity filter. We have compared the x-ray structure of the KcsA K^+ channel with our models. Unlike the helical portions of the pore loops in the K^+ channel, the helical regions of M2s in our models do not have a radial slope. However, this does not affect the major conclusions of the present study that is focused on the structure of the N/Q/R site. In the KcsA K^+ channel, four Thr^{75} residues form a cyclic structure that is remarkably similar to the cyclic structure of the N/Q/R site of GluRs that we predicted earlier (Tikhonov et al., 1998). The distance between the side-chain oxygen of the Thr^{75} residue in a given segment and the main-chain oxygen of the Thr^{75} residue in the adjacent segment is 2.7 Å. This strongly suggests a 24-membered ring (----O-C′-C^{α}-C^{β}-O^{γ}-H^{γ}----)$_4$. The ring is closed in the clockwise direction with the Thr side chain oxygens O^{γ} facing the pore as in our N4c model. Not surprisingly, the predicted diameter of the N/Q/R ring that permeates partially hydrated Ca^{2+} is effectively larger than the inner diameter (about 3.0 Å) of Thr^{75} ring that permeates dehydrated K^+.

The KcsA K^+ channel has Trp^{67} and Asp^{80} residues at the positions homologous to Trp^8 and Asp^{21} residues in

GluR M2. In the x-ray structure of the KcsA K^+ channel, the side chains of these residues form an H-bond $O^{\delta} \cdots H^{\epsilon}$ (Fig. 8 *D*). Our model Q4a-D readily adopts such a structure (Fig. 8 *C*). Thus, our models demonstrate certain three-dimensional homology with the pore region of the KcsA K^+ channel. This evidence is in favor of the tetrameric stoichiometry of GluRs. Future homology modeling of GluRs with the structure of the KcsA K^+ channel used as a template may shed additional light on the structure and function of GluRs.

The authors are thankful to Professor Stuart Edelstein for reading the manuscript and valuable comments. This work is supported by grants 99–04-49815 to BSZ and 99–04-49759 to LGM from the Russian Foundation for Basic Research, and by grant INTAS-RFBR-95–1-11 to LGM.

REFERENCES

Antonov, S. M., J. W. Johnson, N. Y. Lukomskaya, N. N. Potapyeva, V. E. Gmiro, and L. G. Magazanik. 1995. Novel adamantane derivatives act as blockers of open ligand-gated channels and as anticonvulsants. *Mol. Pharmacol.* 47:558–567.

Bennett, J. A., and R. Dingledine. 1995. Topology profile for a glutamate receptor: three transmembrane domains and a channel-lining reentrant membrane loop. *Neuron.* 14:373–384.

Blaschke, M., B. U. Keller, R. Rivosecchi, M. Hollmann, S. Heinemann, and A. Konnerth. 1993. A single amino acid determines the subunit-specific spider toxin block of α-amino-3-hydroxy-5-methylisoxazole-4-propionate/kainate receptor channels. *Proc. Natl. Acad. Sci. USA.* 90: 6528–6532.

Brackley, P. T. H., D. R. Bell, S. K. Choi, K. Nakanishi, and P. N. R. Usherwood. 1993. Selective antagonism of native and cloned kainate and NMDA receptors by polyamine-containing toxins. *J. Pharmacol. Exp. Ther.* 266:1573–1580.

Brovtsyna, N. B., D. B. Tikhonov, O. B. Gorbunova, V. E. Gmiro, S. E. Serduk, N. Y. Lukomskaya, L. G. Magazanik, and B. S. Zhorov. 1996. Architecture of the neuronal nicotinic acetylcholine receptor ion channel at the binding site of *bis*-ammonium blockers. *J. Membr. Biol.* 152: 77–87.

Burnashev, N., H. Monyer, P. H. Seeburg, and B. Sakmann. 1992a. Divalent ion permeability of AMPA receptor channels is dominated by the edited form of a single subunit. *Neuron.* 8:189–198.

Burnashev, N., R. Schoepfer, H. Monyer, J. P. Ruppersberg, W. Gunter, P. H. Seeburg, and B. Sakmann. 1992b. Control by asparagine residues of calcium permeability and magnesium blockade in the NMDA receptor. *Science.* 257:1415–1419.

Burnashev, N., Z. Zhou, E. Neher, and B. Sakmann. 1995. Fractional calcium currents through recombinant GluR channels of the NMDA, AMPA and kainate receptor subtypes. *J. Physiol.* 485:403–418.

Burnashev, N., A. Villarroel, and B. Sakmann. 1996. Dimensions and ion selectivity of recombinant AMPA and kainate receptor channels and their dependence on R/Q site residues. *J. Physiol.* 496:165–173.

Dingledine, R., R. I. Hume, and S. Heinemann. 1992. Structural determinants of barium permeation and rectification in non-NMDA glutamate receptor channels. *J. Neurosci.* 12:4080–4087.

Doyle, D. A., J. M. Cabral, R. A. Pfuetzner, A. Kuo, J. M. Gulbis, S. L. Cohen, B. T. Chait, and R. MacKinnon. 1998. The structure of the potassium channel: basis of K^+ conduction and selectivity. *Science.* 280:69–77.

Ferrer-Montiel, A. V., and M. Montal. 1996. Pentameric subunit stoichiometry of a neuronal glutamate receptor. *Proc. Natl. Acad. Sci. USA.* 93:2741–2744.

Ferrer-Montiel, A. V., W. Sun, and M. Montal. 1995. Molecular design of the *N*-methyl-D-aspartate receptor binding site for phencyclidine and dizolcipine. *Proc. Natl. Acad. Sci. USA.* 92:8021–8025.

Ferrer-Montiel, A. V., W. Sun, and M. Montal. 1996. A single tryptophan on M2 of glutamate receptor channels confers high permeability to divalent cations. *Biophys. J.* 71:749–758.

Ferrer-Montiel, A. V., J. M. Merino, R. Planells-Cases, W. Sun, and M. Montal. 1998. Structural determinants of the blocker binding site in glutamate and NMDA receptor channel. *Neuropharmacology.* 37: 139–147.

Galzi, J. L., and J. P. Changeux. 1995. Neuronal nicotinic receptors: molecular organisation and regulations. *Neuropharmacology.* 34: 563–582.

Geiger, G. R. P., T. Meicher, D. S. Koh, B. Sakmann, P. H. Seeburg, P. Jonas, and H. Monyer. 1995. Relative abundance of subunit mRNAs determines gating and Ca^{2+} permeability of AMPA receptors on principal neurons and interneurons in rat CNS. *Neuron.* 15:193–204.

Herlitze, S., M. Raditsch, J. P. Ruppersberg, W. Jahn, H. Monyer, R. Schoepfer, and V. Witzemann. 1993. Argiotoxin detects molecular differences in AMPA receptor channels. *Neuron.* 10:1131–1140.

Hollmann, M., and S. Heinemann. 1994. Cloned glutamate receptors. *Ann. Rev. Neurosci.* 17:31–108.

Hollmann, M., C. Maron, and S. Heinemann. 1994. N-glycosylation site tagging suggests a three transmembrane domain topology for the glutamate receptor GluR1. *Neuron.* 13:1331–1343.

Kashiwagi, K., A. J. Pahk, T. Masuko, K. Igarashi, and K. Williams. 1997. Block and modulation of *N*-methyl-D-aspartate receptors by polyamines and protons: role of amino acid residues in the transmembrane and pore-forming regions of NR1 and NR2 subunits. *Mol. Pharmacol.* 52: 701–713.

Keinanen, K., W. Wisden, B. Sommer, P. Werner, A. Herb, T. A. Verdoorn, B. Sakmann, and P. H. Seeburg. 1990. A family of AMPA-selective glutamate receptors. *Science.* 249:556–560.

Koh, D. S., G. R. P. Geiger, P. Jonas, and B. Sakmann. 1995. Ca^{2+}-permeable AMPA and NMDA receptor channels in basket cells of rat hippocampal dentate gyrus. *J. Physiol.* 485:383–402.

Kohler, M., N. Burnashev, B. Sakmann, and P. H. Seeburg. 1993. Determinants of Ca^{2+} permeability in both TM1 and TM2 of high affinity kainate receptor channels: diversity by RNA editing. *Neuron.* 10: 491–500.

Koradi, R., M. Billeter, and K. Wuthrich. 1996. MOLMOL: a program for display and analysis of macromolecular structures. *J. Mol. Graph.* 14: 29–32.

Kuner, T., L. P. Wollmuth, A. Karlin, P. H. Seeburg, and B. Sakmann. 1996. Structure of the NMDA receptor channel M2 segment inferred from the accessibility of substituted cysteines. *Neuron.* 17:1–20.

Laube, B., J. Kuhse, and H. Betz. 1998. Evidence for a tetrameric structure of recombinant NMDA receptors. *J. Neurosci.* 18:2954–2961.

Li, Z., and H. A. Scheraga. 1988. Structure and free energy of complex thermodynamic systems. *J. Mol. Struct.* 179:333–352.

Lyle, T. A., C. A. Magill, S. F. Britcher, G. H. Denny, W. J. Thompson, J. S. Murphy, A. R. Knight, J. A. Kemp, J. R. Marshall, D. N. Middlemiss, E. H. F. Wong, and P. S. Anderson. 1990. Structure and activity of hydrogenated derivatives of (+)-5-methyl-10,11-dihydro-5H-dibenzo[a,d]cyclohepten-5,10-imine (MK-801). *J. Med. Chem.* 33: 1047–1052.

Magazanik, L. G., S. L. Buldakova, M. V. Samoilova, V. E. Gmiro, I. R. Mellor, and P. N. R. Usherwood. 1997. Block of open channels of recombinant AMPA receptors and native AMPA/kainate receptors by adamantane derivatives. *J. Physiol.* 505:655–663.

Manallack, D. T., M. G. Wong, M. Costa, P. R. Andrews, and P. M. Beart. 1988. Receptor site topographics for phencyclidine-like and delta drugs: predictions from quantitative conformational, electrostatic potential, and radio-receptor analysis. *Mol. Pharmacol.* 34:863–879.

Mano, I., and V. I. Teichberg. 1998. A tetrameric subunit stoichiometry for a glutamate receptor-channel complex. *Neuroreport.* 9:327–331

Mayer, M. L., and G. L. Westbrook. 1987. Permeation and block of *N*-methyl-D-aspartic acid receptor channels by divalent cations in mouse cultured central neurons. *J. Physiol.* 394:501–527.

Momany, F. A., R. F. McGuire, A. W. Burgess, and H. A. Scheraga. 1975. Energy parameters in polypeptides. VII. Geometric parameters, partial atomic charges, nonbonded interactions, hydrogen bond interactions, and intrinsic torsional potentials of the naturally occurring amino acids. *J. Phys. Chem.* 79:2361–2381.

Mori, H., H. Masaki, T. Yamakura, and M. Mishina. 1992. Identification by mutagenesis of a Mg^{2+}-block site of the NMDA receptor channel. *Nature.* 358:673–675.

Nemethy, G., M. S. Pottle, and H. A. Scheraga. 1983. Energy parameters in polypeptides. 9. Updating of geometrical parameters, nonbonded interactions, and hydrogen bond interactions for the naturally occurring amino acids. *J. Phys. Chem.* 87:1883–1887.

Rosenmund, C., Y. Stern-Bach, and C. F. Stevens. 1998. The tetrameric structure of a glutamate receptor channel. *Science.* 280:1596–1599.

Ruppersberg, J. P., J. Mosbacher, W. Gunter, R. Schoepfer, and B. Fakler. 1993. Studying block in cloned *N*-methyl-D-aspartate (NMDA) receptors. *Neuropharmacology.* 46:1877–1885.

Sankararamakrishnan, R., and M. S. P. Sansom. 1995. Water-mediated conformational transitions in nicotinic receptor M2 helix bundles: a molecular dynamics study. *FEBS Lett.* 377:377–382.

Seeburg, P. H. 1993. The TIPS/TINS lecture: the molecular biology of mammalian glutamate receptor channels. *Trends Pharmacol. Sci.* 14: 297–303.

Sussman, J. L., M. Harel, and I. Silman. 1993. Three-dimensional structure of acetylcholinesterase and of its complexes with anticholinesterase drugs. *Chem. Biol. Interact.* 87:187–197.

Sutcliffe, M. J., Z. G. Wo, and R. E. Oswald. 1996. Three-dimensional models of non-NMDA glutamate receptors. *Biophys. J.* 70:1575–1589.

Swanson, G. T., D. Feldmeyer, M. Kaneda, and S. G. Cull-Candy. 1996. Effect of RNA editing and subunit co-assembly on single-channel properties of recombinant kainate receptors. *J. Physiol.* 492:129–142.

Swanson, G. T., S. K. Kamboj, and S. G. Cull-Candy. 1997. Single-channel properties of recombinant AMPA receptors depend on RNA editing, splice variation, and subunit composition. *J. Neurosci.* 17:58–69.

Tikhonov, D. B., and B. S. Zhorov. 1998. Kinked-helices model of the nicotinic acetylcholine receptor ion channel and its complexes with blockers: simulation by the Monte Carlo minimization method. *Biophys. J.* 74:242–255.

Tikhonov, D. B., B. S. Zhorov, and L. G. Magazanik. 1998. Common structure and specific features of glutamate receptor channels: molecular modeling. *J. Neurochem.* 71(Suppl):S88B.

Unwin, N. 1995. Acetylcholine receptor channel imaged in the open state. *Nature.* 373:37–43.

Villarroel, A., N. Burnashev, and B. Sakmann. 1995. Dimensions of the narrow portion of a recombinant NMDA receptor channel. *Biophys. J.* 68:866–875.

Washburn, M. S., and R. Dingledine. 1996. Block of alpha-amino-3-hydroxy-5-methyl-4-isoxazolepropionic acid (AMPA) receptors by polyamines and polyamine toxins. *J. Pharmacol. Exp. Ther.* 278: 669–678.

Washburn, M. S., M. Numberger, S. Zhang, and R. Dingledine. 1997. Differential dependence on GluR2 expression of three characteristic features of AMPA receptors. *J. Neurosci.* 17:9393–9410.

Wenthold, R. J., N. Yokotani, K. Doi, and K. Wada. 1992. Immunochemical characterization of the non-NMDA glutamate receptor using subunit-specific antibodies. Evidence for a hetero-oligomeric structure in rat brain. *J. Biol. Chem.* 267:501–507.

Westbrook, G. L. 1994. Glutamate receptor update. *Cur. Opin. Neurobiol.* 4:337–346.

Williams, K., A. J. Pahk, K. Kashiwagi, T. Masuko, N. D. Nguyen, and K. Igarashi. 1998. The selective filter of the *N*-methyl-D-aspartate receptor: a tryptophan residue controls block and permeation of Mg^{2+}. *Mol. Pharmacol.* 53:933–941.

Wo, Z. G., and R. E. Oswald. 1994. Transmembrane topology of two kainate receptor subunits revealed by N-glycosilation. *Proc. Natl. Acad. Sci. USA.* 91:7154–7158.

Wollmuth, L. P., T. Kuner, P. H. Seeburg, and B. Sakmann. 1996. Different contribution of the NR1- and NR2-subunits to the selectivity filter of recombinant NMDA receptor channels. *J. Physiol.* 491:779–797.

Wollmuth, L. P., T. Kuner, and B. Sakmann. 1998. Adjacent asparagines in the NR2-subunit of the NMDA receptor channel control the voltage-dependent block by extracellular Mg^{2+}. *J. Physiol.* 506:13–32.

Wollmuth, L. P., and B. Sakmann. 1998. Different mechanisms of Ca^{2+} transport in NMDA and Ca^{2+}-permeable AMPA glutamate receptor channels. *J. Gen. Physiol.* 112:623–636.

Wood, M. W., H. M. A. VanDongen, and A. M. J. VanDongen. 1995. Structural conservation of ion conduction pathways in K channels and glutamate receptors. *Proc. Natl. Acad. Sci. USA.* 92:4882–4886.

Wu, T. Y., C. I. Liu, and Y. C. Chang. 1996. A study of the oligomeric state of the alpha-amino-3-hydroxy-5-methyl-4-isoxazolepropionic acid-preferring glutamate receptors in the synaptic junctions of porcine brain. *Biochem. J.* 319:731–739.

Wyllie, D. J., P. Behe, M. Nassar, R. Schoepfer, and D. Colquhoun. 1996. Single-channel currents from recombinant NMDA NR1A/NR2D receptors expressed in *Xenopus* oocytes. *Proc. R. Soc. B.* 263:1079–1086.

Zarei, M. M., and J. A. Dani. 1995. Structural basis for explaining open-channel blockade of the NMDA receptor. *J. Neurosci.* 15:1446–1454.

Zhorov, B. S. 1981. Vector method for calculating derivatives of energy of atom–atom interactions of complex molecules according to generalized coordinates. *J. Struct. Chem.* 22:4–8.

Zhorov, B. S., and V. S. Ananthanarayanan. 1996. Structural model of synthetic Ca^{2+} channel with bound Ca^{2+} ions and dihydropyridine ligand. *Biophys. J.* 70:22–37.